國 立 交 通 大 學

電子工程學系電子研究所

碩 士 論 文

鎳-磷-鑽石奈米複合材料之複合效應於材料特性差異上的研究

The Investigation of Property Distinction in Ni-P-Diamond Nanocomposite System

研 究 生：蔣 宜 達

指導教授：鄭 裕 庭　教授

中 華 民 國 九 十 五 年 一 月

鎳-磷-鑽石奈米複合材料之複合效應於材料特性差異上的研究

The Investigation of Property Distinction in Ni-P-Diamond Nanocomposite System

研 究 生：蔣宜達　　Student：I-Ta Chiang

指導教授：鄭裕庭　　Advisor：Yu-Ting Cheng

國 立 交 通 大 學

電子工程學系電子研究所

碩 士 論 文

A Thesis

Submitted to Department of Electronics Engineering & Institute of Electronics

College of Electrical Engineering and Computer Science

National Chiao-Tung University

in Fulfillment of the Requirements

for the Degree of

Master

in

Electronics Engineering

July 2004

Hsinchu, Taiwan, Republic of China

中華民國九十五年一月

鎳-磷-鑽石奈米複合材料之複合效應於材料特性差異上的研究

學生：蔣宜達　　指導教授：鄭裕庭教授

國立交通大學電子工程系暨電子研究所碩士班

摘　　要

先前我們已經發表過在鎳基材中摻入如二氧化矽、鑽石、碳管等奈米微粒可以改變鎳金屬的機、電特性。這些特性的改善使得奈米複合材料在微機電的應用上具有很大的發展性。為了更進一步的應用這些奈米複合材料、有效控制材料特性來製作元件，我們必需對複合材料特性做更深入的研究，了解在奈米微粒不同粒徑、外型及在基材中不同的分佈情形時所造成的特性差異。到目前為止，只有少數的研究針對這些問題去做探討。在本篇論文中將報告一個在鎳-磷-鑽石奈米複合材料中觀察到的有趣現象，即在摻雜相同的二相材料進入不同微結構的鎳基材時將產生不同的材料特性變化。奈米壓痕儀的量測結果指出，在奈米鑽石微粒體積百分比 4%含量下且微結構為非晶型態的鎳-磷-鑽石複合材料薄膜其硬度值從純鎳-磷薄膜的 6.7GPa提升到 7.5GPa，反觀微結構由非晶及奈米晶粒所組成的鎳-磷-鑽石薄膜其硬度值隨著奈米鑽石微粒含量的增加能下降。同時，量測每公升鍍液裡有 2 克的奈米鑽石微粒溶液中鍍出來的鎳-磷-鑽石複合材料薄膜

電性可以發現，非晶結構的鎳-磷-鑽石複合材料比微結構為非晶及奈米晶粒所組成的鎳-磷-鑽石複合材料有更好的導電性，其相對應的量測電阻率分別為 $1.125*10^{-6}\Omega$-m及 $1.561*10^{-6}\Omega$-m。另一方面，由鎳-磷-鑽石複合材料所製成的電熱式微致動器，無論在何種微結構下其最大位移量均比由純鎳-磷材料所製成的微致器來的大，此外，非晶型態的鎳基材電熱式微致動器比微結構為非晶及奈米晶粒所組成的鎳基材微致動器有更佳的電源效率。我們相信這些觀察到的現象將引起材料學者及元件工程師在複合材料的理論研究及應用上的興趣。

The Investigation of Property Distinction in Ni-P-Diamond Nanocomposite System

Student : I-Ta Chiang Advisor : Yu-Ting Cheng

Department of Electronics Engineering & Institute of Electronics

National Chiao Tung University

Abstract

Previously, we have reported that incorporating nanoparticles, such as SiO_2, diamond, and carbon nanotube (CNT) into a nickel matrix can change the mechanical and electrical properties of pure nickel. The property modifications have shown a great potentiality of the nanocomposites for MEMS applications. However, for the advancement of the applications, it is required to further investigate on the material property modification resulted by nanocomposite effects, such as particle size, shape, and distribution effects on the matrix, from which the material properties can be well engineered for designated device fabrication. So far, few researches have been worked on the related issues. In the thesis, an interesting phenomenon is observed and reported in Ni-P-Diamond nanocomposite system, in which the microstructure difference of Ni matrix would result in distinct property modifications even though the same second phase material is added. The nanoindentation measurement shows that the Young's modulus and harness of the amorphous

crystallization of the Ni-P films can increase from 6.7Gpa to 7.5Gpa while 4% volume fraction of nano-diamonds are incorporated. In contrast, the modulus and hardness of the Ni-P films with a mixed microstructure of nanocrystalline and amorphous phase decrease with the incorporation of the nano-diamonds. Meanwhile, from the electrical measurements of the 2g/L Ni-P-Diamond nanocomposite films, it is found that the resistivities of these two Ni-P-Diamond nanocomposites are $1.125*10^{-6}\Omega$-m and $1.561*10^{-6}\Omega$-m, respectively for an amorphous matrix and a matrix with the mixtures of nanocrystalline and amorphous phase, which indicating the Ni-P-Diamond nanocomposite with amorphous Ni matrix has better electrical conductivity than the other. Since it is found that the electrothermal microactuator made of both Ni-P-Diamond nanocomposites can exhibit a larger ultimate elongation than that made of pure Ni-P and the actuator made of the nanocomposite with fully amorphous Ni matrix can have a better power-efficient performance as compared, it is our belief that the observations would lead a great interest to material scientists and device engineers in the future development of nanocomposite synthesis and theory.

誌　謝

首先，我要感謝的家人，爸爸、媽媽、還有弟弟，謝謝你們在這段期間對我精神上、生活上的支持，對於一個快 30 歲的人還沒辦法對家裡有所貢獻，反而還需要你們的支助，我真的很感謝，家人永遠是最好的支持者，我很慶興有你們當家人。爸、媽，現在我畢業了，我和阿興將盡力讓你們過安祥舒適的日子，畢竟你們為這個家辛苦了一輩子，是該好好休息一下換我和阿興接手了。

此外，我要感謝我的指導老師鄭裕庭教授，謝謝你在這段期間對我的指導，謝謝!!另外，我還要感謝交大材料所蔡欣瑩小姐及陳曉雲學姐，謝謝你們對一個完全不相干的人伸出援手，幫我做量測，非常感謝。

當然我還要跟我們實驗室的伙伴們說聲謝謝，學姐、光仁、志瑋、凱哥、子元、健章、chando、小 b、思穎、昱文還有過很爽的助理小筑^^，謝謝大家有共同的目標，能一起哈啦打屁、發洩心情，剩下來的看你們了，加油吧，忍一忍、撐一下就過了，大家的目標都一樣，光仁他們是如此，我們也是如此，你們也一樣，不過我能說的，也只是~~~加油。

最後我要謝謝另一個在背後支持我的人，我的女朋友怡青，謝謝你陪我走過來，聽我訴苦，也很抱歉這段日子都沒帶你出去玩，歹勢啦^^|

宣告：給我的豬朋狗友們，別再問我到底什麼時候要畢業了，別再說我變遜了，我沒變遜，我畢業了，我的階段任務完成了，我回來了，雖然我知道你們現在薪水都上 50k 了，但我會努力追上你們的，小心啦~~~~

Contents

Figure Captions

Chapter 2

Chapter 3

Table Captions

Chapter 1

Chapter 3

Chapter 1 Introduction

In the contemporary fabrication process of microelectromechanical system (MEMS) devices, the polysilicon and metal, such as Cu, Al, and Ni, are the main materials due to their excellent mechanical and electrical properties. But these materials are existence some deficiency. For example, the highly-doped polysilicon deposition should be processing under high temperature (>1000℃) environment, this processing temperature makes itself not suitable for CMOS integration. In addition, the metal materials have aging and fatigue issues. Table 1-1 shows the advantages and disadvantages of these materials. In order to practice a post-COMS MEMS integration, it is necessary to develop a low temperature process. Base on this, we have proposed a selective electroless nanocomposite deposition techniques [1,2,3] previously. We had successfully used Ni-base nanocomposites to make a MEMS device that the device can be made below 100℃ and also have good properties.

Utilizing the structure material with second phase effects to enhance device performance makes nanocomposite materials fascinating in recent nanotechnology development. Various metal/ceramic nanocomposites have been synthesized and proposed for potential applications such as tribological coating, gas sensing, and RF [4,5,6]. A metal incorporated with well distributed ceramic nanopowders like Al_2O_3, Si_3N_4, SiO_2, diamond, and Fe(II, III) oxide can have homogeneous material property modification including the augment of hardness,

Young's modulus, coefficient of thermal expansion (CTE), or coercivity that is beyond its intrinsic characteristic limit. Since it has been found that the residual stress of nanocomposite film can also be customized with adequate incorporation of nanoparticles for the fabrication of microactuators, related investigations on property characterization become critical for further applications.

Previously, we have many investigations on the Ni-based nanocomposite, but all of that are focused on second phase effects. However, many investigations have been reported that the phosphorus contents of the EN films can effect upon the crystallization and microstructural properties. [7,8,9] Based on phosphorus contents, the electroless nickel (EN) deposits can classified as low (1~5 wt% P), medium (5~9 wt% P) and high (>9 wt% P) phosphorus content. Table 1-2 shows that the crystallization on different phosphorus contents. Therefore, in this thesis, we will report an interesting phenomenon observed in Ni-P-diamond nanocomposite systems. Totally distinct nanocomposite effects on the material property enhancement resulted by the difference of matrix microstructure are found even though the matrix and secondary phase materials are the same.

Table 1-1 The advantage and disadvantage of the polysilicon and metal materials in MEMS application.

	Polysilicon	Metal
Advantage	1.Good mechanical properties 2.CTE close to Si substrate	1.Low fabrication temperature 2.Good electrical conductivity
Disadvantage	1.High fabrication temperature 2.High resistivity	1.Aging and fatigue problem 2.CTE mismatch to Si substrate 3.Residual stress problem

Table 1-2 Relationship between the crystallization and the phosphorus contents of EN films.[8,10-12]

	Phosphorus contents (wt%)	Crystallization
Low	1~5	1.Crystalline 2.Consist of microcrystalline nickel
Medium	5~9	1.Fully amorphous 2.Mixtures of microcrystalline nickel and amorphous
High	9 and above	1.Fully amorphous 2.Mixtures of microcrystalline nickel and amorphous 3.Consist of 2 and various other phases such as Ni_5P_4, $Ni_{12}P_5$, Ni_5P_2

Chapter 2 Concept Design and Sample Preparation

2.1 Concept Design of the Electrothermal Microactuator

The electrothermal microactuator is based on the long-short beam design [13] as shown in Fig. 2-1. The device structure is consists of two anchor pads and a pair of adjacent cantilever beams with different lengths that connect in one end. By resistively heating these two beams, unequal thermal expansions make the joint of the beams toward to the shorter one and provide a lateral actuation. In our design, the length of the long beam is 800μm and the short beam is 400μm, both beams wide and the gap between these two beams are 10μm. With the fixed plating parameter, the thickness of the actuator is about 7μm

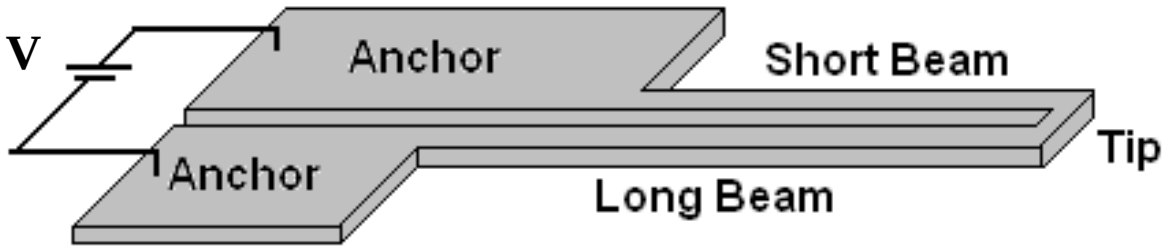

Fig. 2-1 The Concept Design of an Electro-Thermal Microactuator.[13]

2.2 Sample Preparation

2.2.1 Electroless Ni-P-Diamond Plating Solution Preparation

To make a good Ni-P electroless thinfilm or devices, the plating solution is an important point to attention, because some commercial plating solution would cause deposited surface rough. As the Ni-P-Diamond electroless plating, well dispersed diamond powders can ensure the powders uniformly engulfed into nickel matrix during the processing. In our study, prepare of 1 liter Ni-P-Diamond plating bath, a commercial Ni-P plating bath [14] composed of 150mL Sheng-Hung chemical nickel plating SCNP A solution and 150mL SCNP B solution is first mixed with prewetted diamond powder (average size<0.5μm, density: 3.51g/cm^3) solution. Then utilize D.I. water and NH_4OH to modify the pH value to 4.6 and make the total solution volume 1 liter. During plating process, good stir of the plating solution can keep the diamond powders dispersive well for uniform deposition of Ni-P-Diamond nanocomposite. The plating solution with different diamond concentrations are premeditated to characterize fabrication process and material property, which are 0, 0.5, 1, and 2 gram of the diamond powders per liter of plating solution, respectively. Fig. 2-2 illustrate the total setup of the electroless plating equipment.

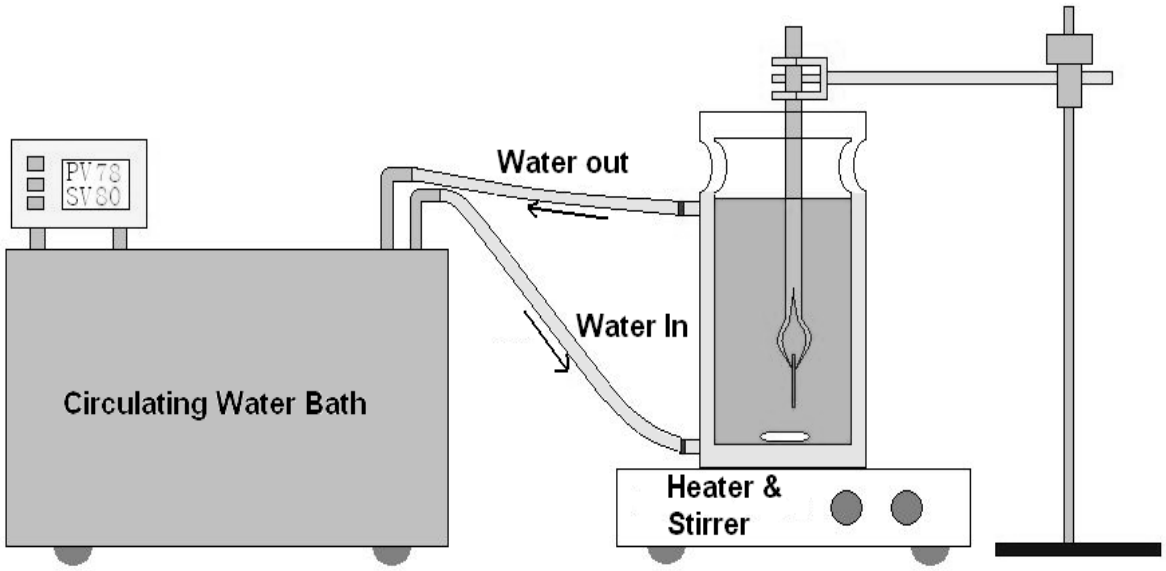

Fig. 2-2 The electroless plating equipments setup.[15]

2.2.2 Fabrication Process of the Electrothermal Microactuator

The electrothermal microactuator structure is shown in Fig. 2-1. The fabrication process flow described in below, and the Fig. 2-3 is the relative process flow chart.

Step1: After standard RCA clean, a 2μm HDP-CVD SiO_2 is deposited on the 4 inch silicon wafer as the electrical insulation and sacrificial layer.

Step2: Sputter a Ti/Cu (100Å/500Å) seed layer on the top of the SiO_2.

Step3: Coating a 10μm thick AZP-4620 photoresist (PR) to mold the device structure.

Step4: Put the wafer into the Pd seeding solution for 30seconds to active the copper surface. After being seeded, the wafer put into the Ni-P or the Ni-P-Diamond plating bath for 7μm thick nanocomposite film deposition. During the plating process, the temperature of plating bath is kept at 78℃ and also kept the plating solution circulation well.

Step5: Released the structure. First, utilize the acetone and $NH_4OH+H_2O_2$ to removal the mold of PR AZP-4620 and copper seed layer. Then, by dipping the wafer into HF to etch the Ti seed layer and the SiO_2 sacrificial layer under the beams. In order to prevent the suspending structure sticktion, after the structure released, put the wafer into the IPA and then baked at 90℃. Finally, the device is done.

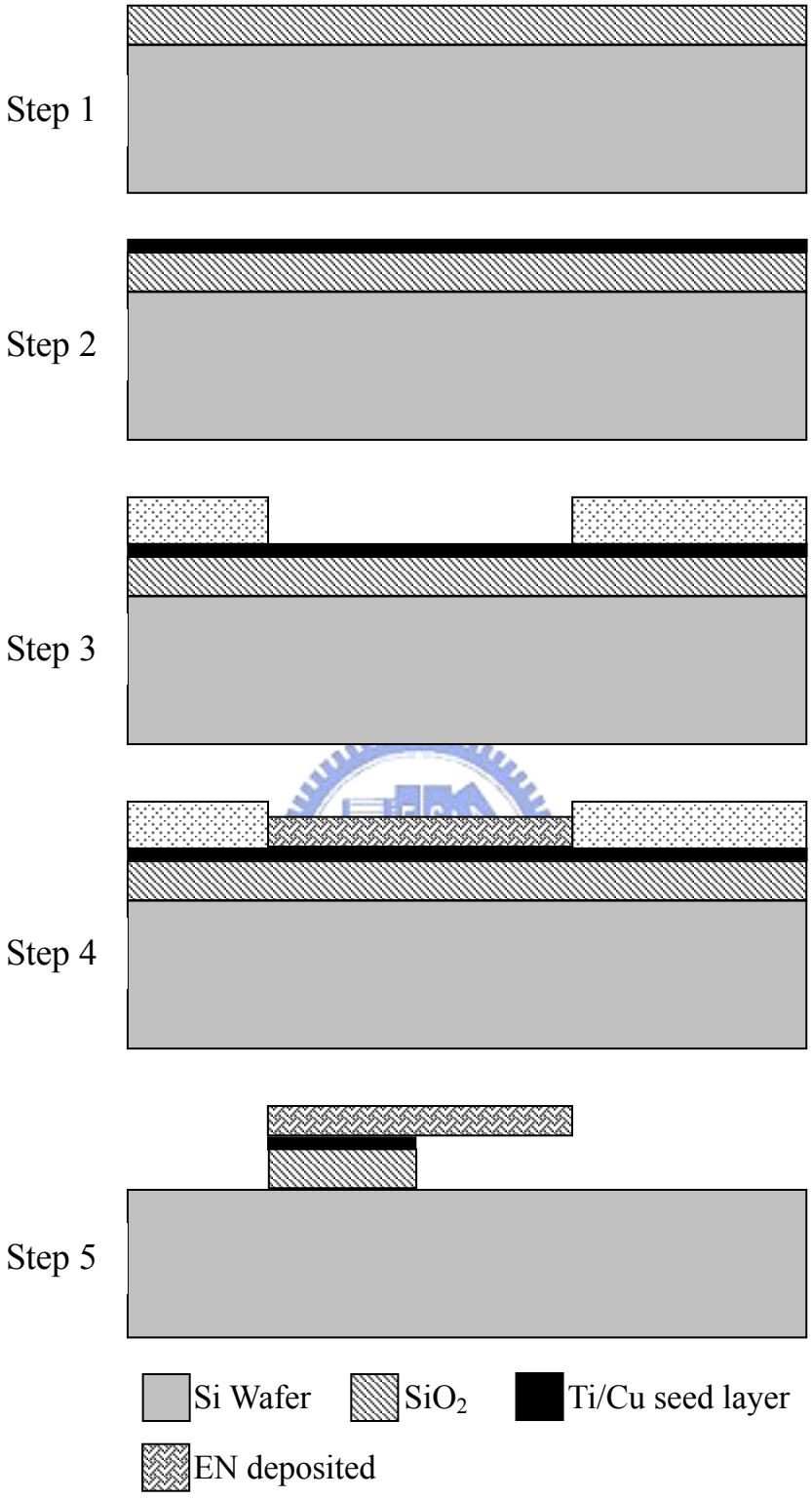

Fig. 2-3 The electrothermal microactuator process flow chart.

Chapter 3 Results and Discussions

In this chapter, we will report the properties which we observe in Ni-P-Diamond nanocomposite that has different matrix microstructure. In order to easy for the report and discussion later, here we define:

Case 1 represents the fully amorphous phase crystallization.

Case 2 represents the mixtures of microcrystalline nickel and amorphous phase crystallization.*

* The data about case 2 are extracted from Shen's thesis. [15]

3.1 The SEM photograph

The Scanning Electro Microscope (SEM) photograph of the Ni-P-Diamond nanocomposite deposition surface and electrothermal microactuator are shown in the Fig. 3-1 and Fig. 3-2. Based on the Fig. 3-1, we can confirm that the diamond powder is embedded in the nickel matrix. Furthermore, Fig. 3-1(b) shows that the case 2 of Ni-P-Diamond nanocomposite deposition has some cracks and voids; it is not our desired because the defect would result in bad properties of nanocomposite.

3.2 Phosphorus content and Crystallization analysis

Many investigations have been reported that the phosphorus contents of the electroless nickel films can effect upon the crystallization and microstructural properties. Also we believe, the phosphorus content will effect on the property

of the electroless nickel based nanocomposite. Therefore, ensure the phosphorus content in the Ni-P-Diamond is very important in this study. The Energy Dispersive Spectroscopy (EDS) is utilized to analyze phosphorus content of the Ni-P-Diamond nanocomposite deposition. By EDS analyze, the phosphorus content is 7.32wt% and 7.11wt% respectively corresponding to the case 1 and case 2. Both of two cases are taken into medium phosphorus content class. Fig. 3-3 shows the EDS diagram. Through the EDS diagram, the carbon peaks indicate again that the diamond powder is real existence in the Ni-P-Diamond nanocomposite deposition.

The X-ray diffractometer, PHILIPS X'Pert Pro (MRD) is utilized to analyze the crystallization of the EN-based depositions. The XRD profiles of the case 1 and 2 are shown in Fig. 3-4. In the Fig. 3-4(b), the Ni(111) peak appear at the angle about 44.8°, and the broad width peak of the amorphous Ni phase is also revealed and overlapped with the Ni(111) microcrystalline peak. Compare the X-ray profiles between the case 1 and case 2, the data show that they are different matrix microstructure. However, the amorphous phase will transform into crystalline after the high temperature annealing. But it is no any annealing process in our study, because the working temperature is not suitable for post –COMS MEMS integration.

By the EDS and X-ray data, we can see that it is different crystallization in the medium phosphorus content. It is conformed to other investigated report.

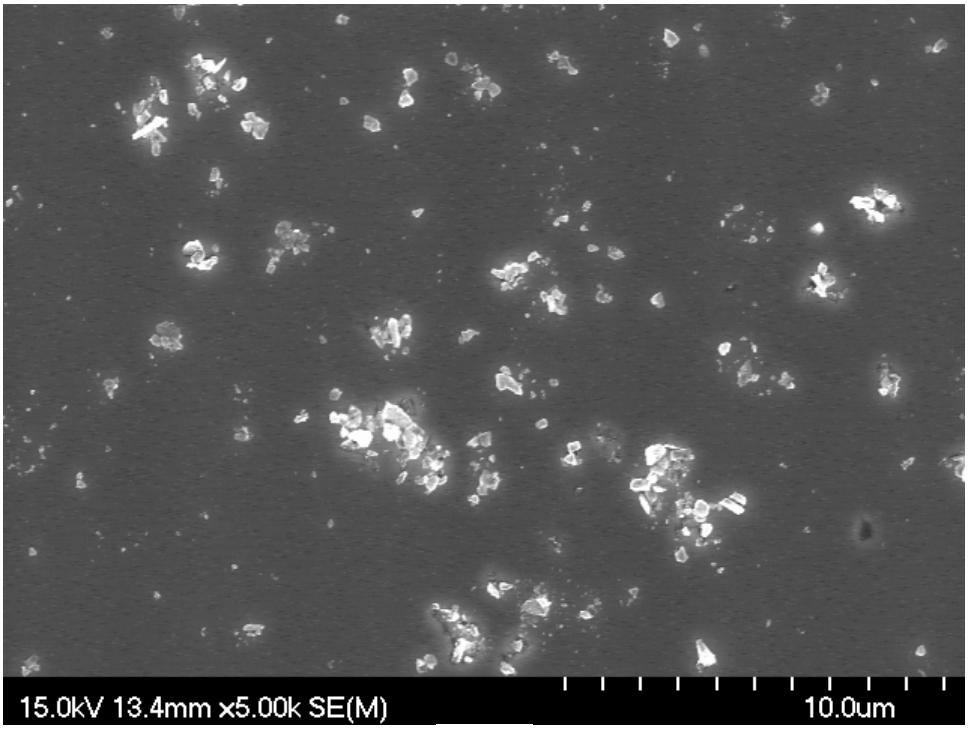

(a)

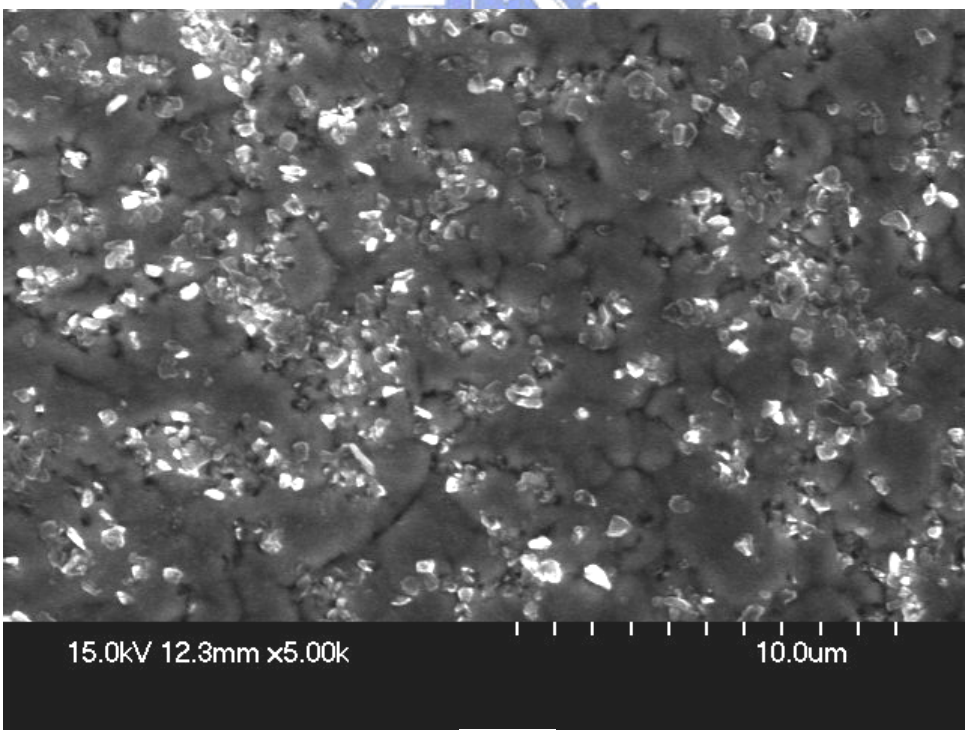

(b)

Fig. 3-1 The SEM photo of Ni-P-Diamond deposition surface
(a) case 1 (b) case 2

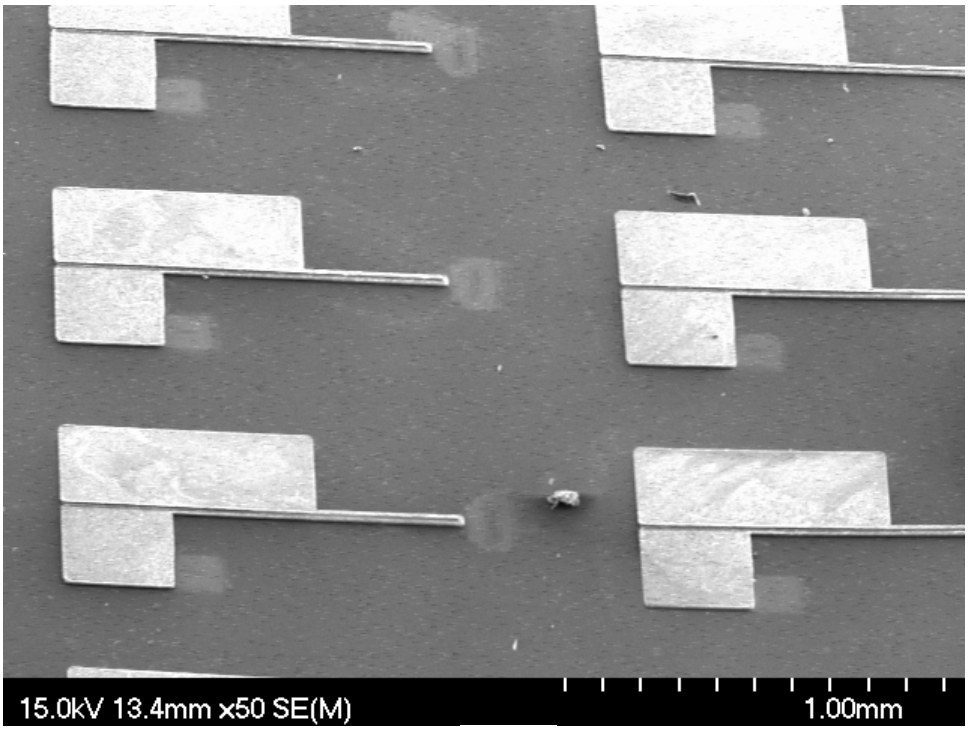

(a)

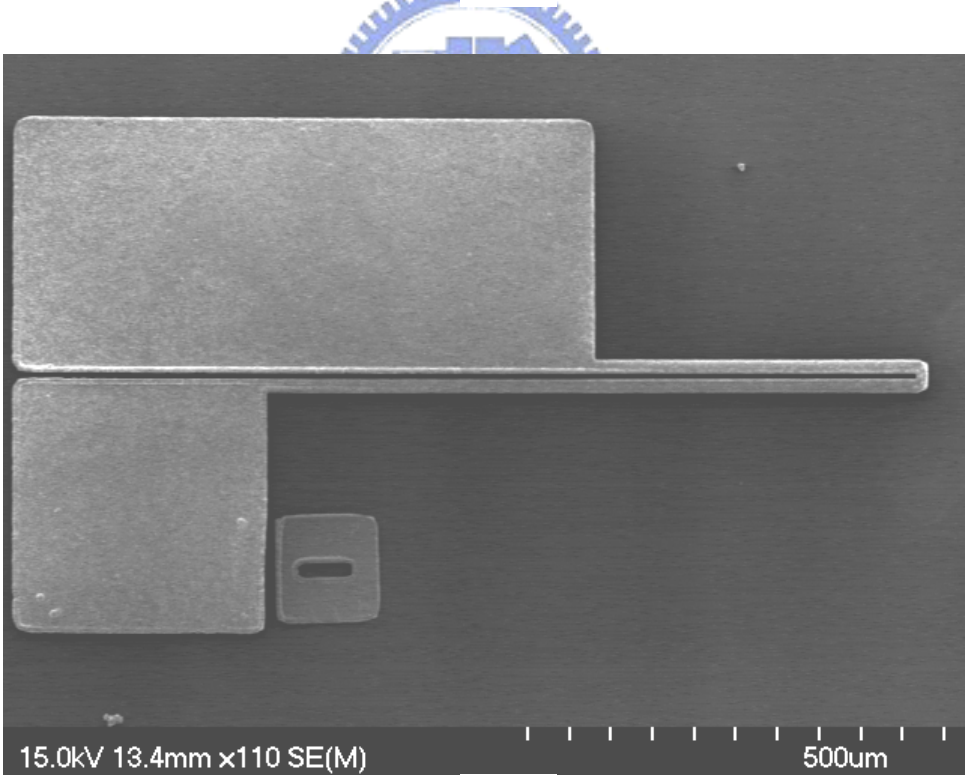

(b)

Fig. 3-2 (a) (b) The fabricated electrothermal microactuator.

(a)

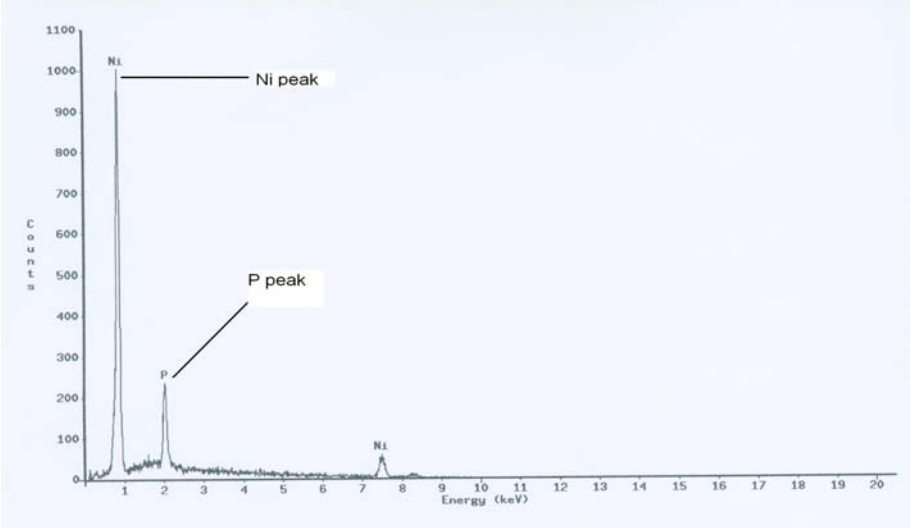

(b)

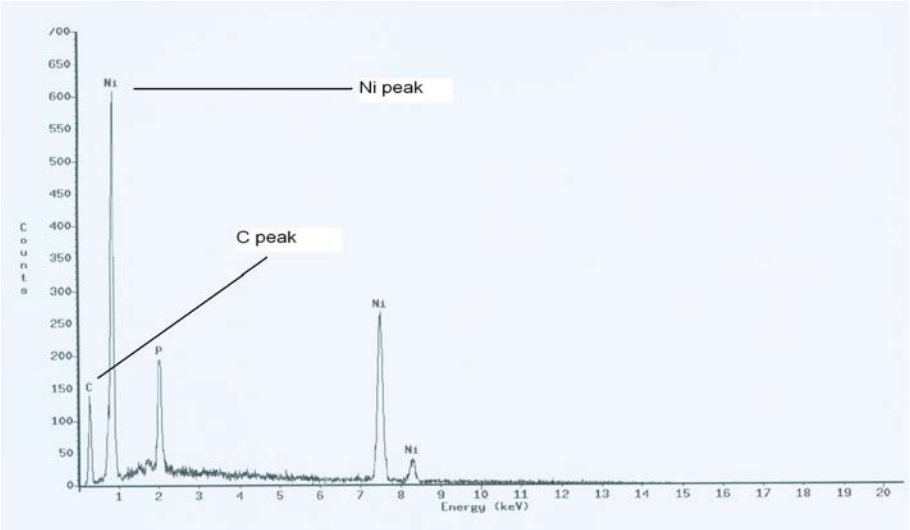

(c)

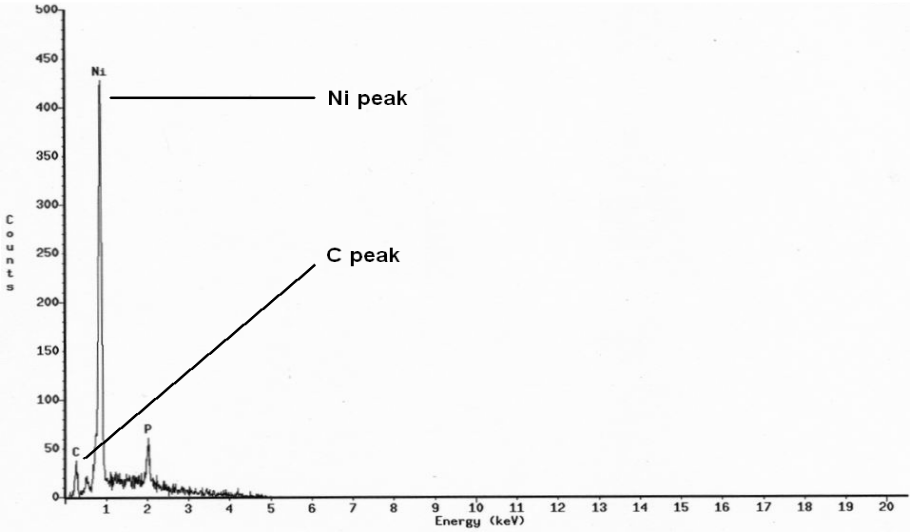

Fig. 3-3 The EDS diagram. (a) pure Ni-P film (b) case 1of the Ni-P-Diamond film (c) case 2 of Ni-P-Diamond film

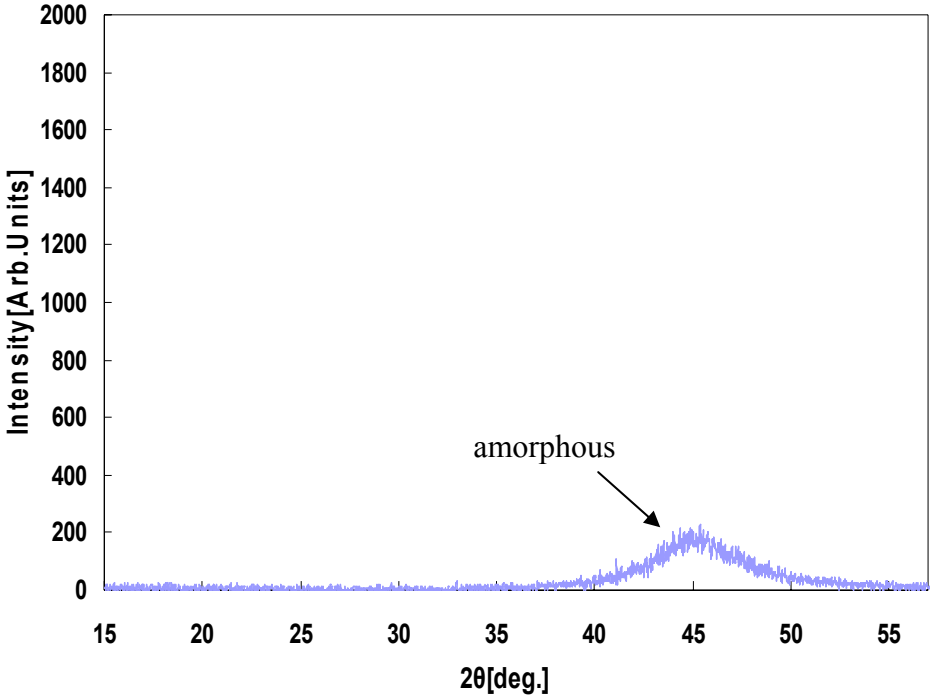

(a)

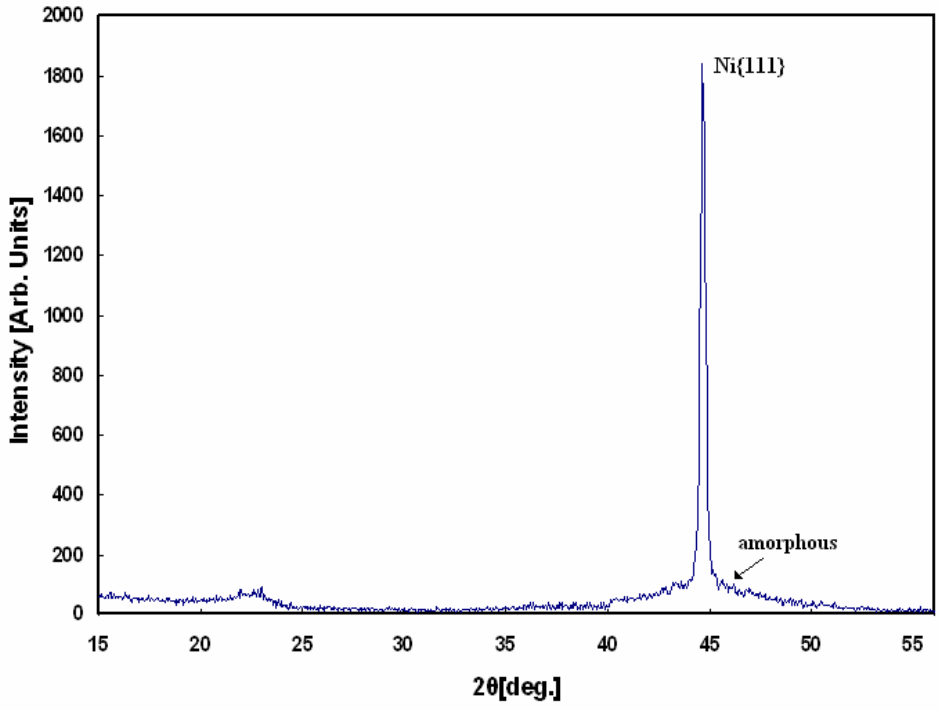

(b)

Fig. 3-4 The X-ray diffraction profile. (a) case 1 (b) case 2

3.3 The Element Analyzer (EA) Analysis

The volume fractions of diamond powders within Ni-P-Diamond deposit should be conformed to make a further comparison and discussion for various measurements. With EA analysis, the weight fractions of the diamond powders in the Ni matrix can be corroborated. Then the volume fractions of diamond powders in the deposit can be obtained by the variables transformation from the density of nickel (8.908g/cm^3) and the density of diamond powder (3.51g/cm^3). The weight fractions and volume fractions of the diamond powders in the Ni-P-Diamond films are shown in Table 3-1. Fig. 3-5 shows the diagrams of volume fractions of diamond powders versus the concentrations of the plating bath. We can see that with the same process conditions, more diamond powders which is two times of that in case 1 can be contained in case 2. By this data and SEM graphics shown in Fig. 3-1, we can observe that too many diamond powders content would cause the deposit results crack, what's influence resulted from this defect will observe by Nano-Indentation test and discussion after.

Table 3-1 The measured weight fractions and volume fractions of two cases with different diamond concentrations.

	Case 1 -Diamond concentration (g/L)				Case 2 -Diamond concentration (g/L)			
	0	0.5	1	2	0	0.5	1	2
Weight fraction	0%*	0.84%	0.93%	1.55%	0%*	1.58%	1.84%	2.72%
Volume fraction	0%	2.15%	2.38%	4%	0%	4.06%	4.76%	7.08%

*The actuality measure value is 0.05%.

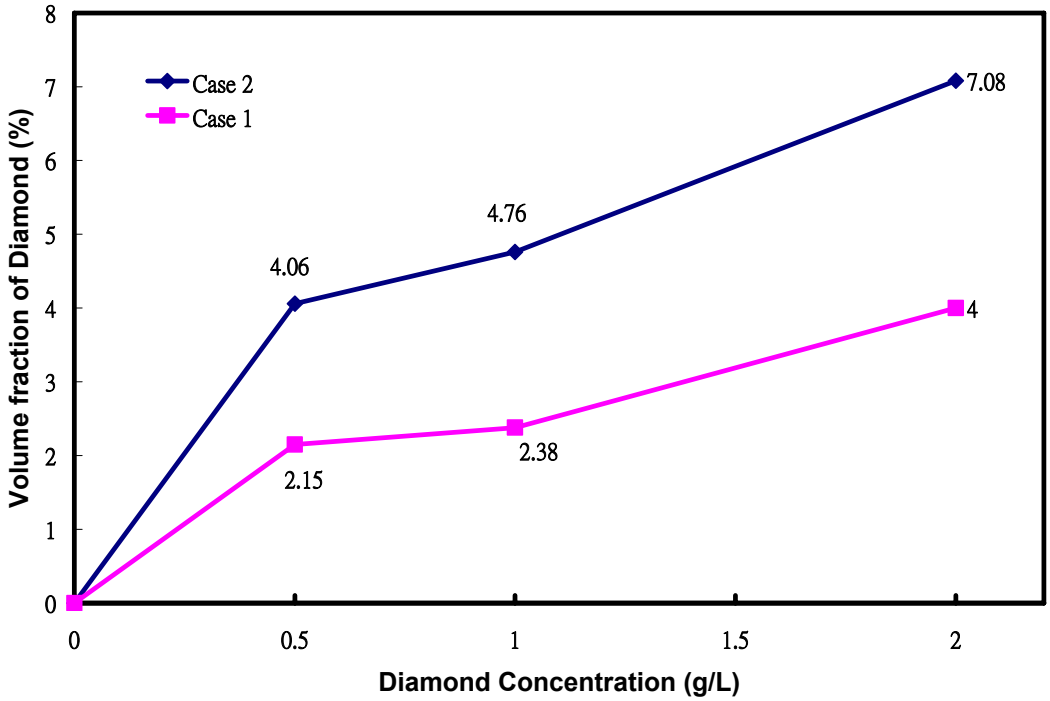

Fig. 3-5 The plot of diamond volume fractions versus plating bath concentrations.

3.4 The Nano-Indentation tests

For the characterization of nanocomposite effects, the Ni-P-Diamonds films are deposited in EN-based solutions with different concentrations of diamond powders, which are 0, 0.5, 1, 2g/L, respectively. For case 1, Fig. 3-6 and Fig. 3-7 show the Young's modulus and hardness values of nano-indentation test results. Here the Rule of Mixtures (ROM) [16,17] can be applied to estimate the physical properties of the composite material. According to the rule, the effective Young's modulus of the Ni-P-Diamond has the upper-bound and low-bound values that are estimated as:

$$E_{eff} = E_c f_c + E_m f_m \qquad \text{for the upper-bound}$$

$$E_{eff} = \frac{E_m E_c}{E_m f_c + E_c f_m} \qquad \text{for the lower-bound}$$

Where E_c, f_c, E_m and f_m are the Young's modulus and volume fraction of the diamond powder and nickel matrix, respectively. The theoretical value of E_c is 1100GPa for diamond and the volume fraction is shown in Table 3-1. The measurement and estimate values of case 1 and case 2 are show in Fig. 3-8. The data shows that the measured Young's modulus is more close to the Low-bound in case 1. It is due to the relative modulus ratio (E_c/E_m) is high and low volume fraction of the diamond powders, so the effective modulus is approach that of the Ni matrix. Similar study has been reported in Kim's research. [18] Also we can see that compared to the pure Ni-P film, hardness value increases in case 1 but decreases in case 2 with increase the diamond powders content. This difference may result from cracks and voids. However, compared with the case 1 and case 2, the case 1 has better mechanical strength then suitable for device applications.

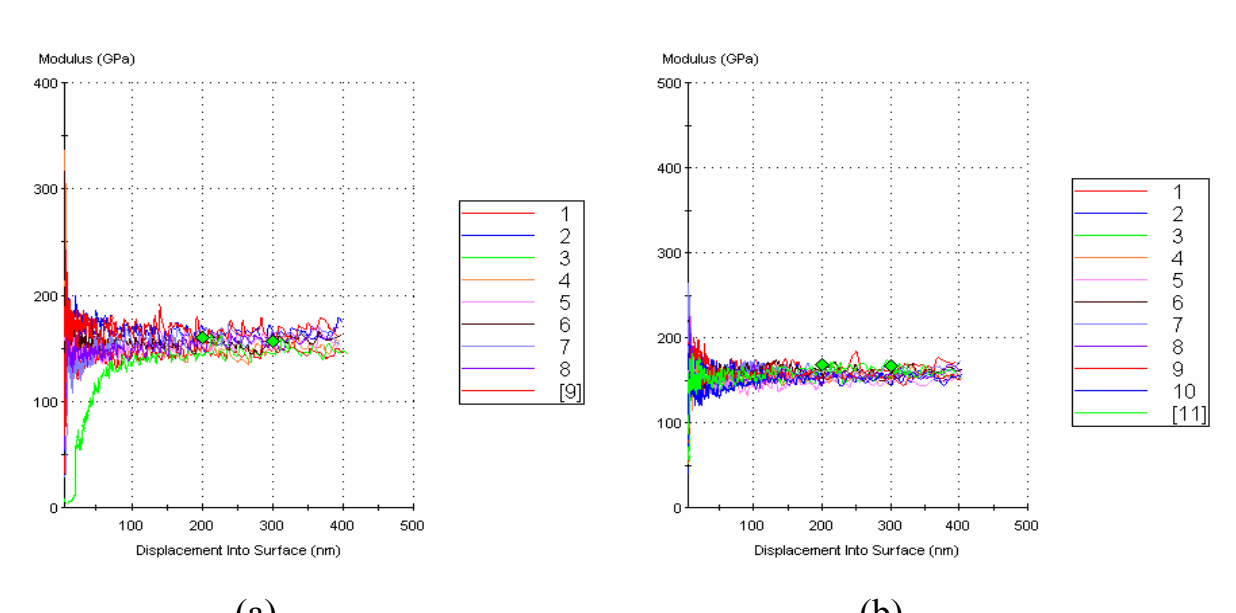

(a) (b)

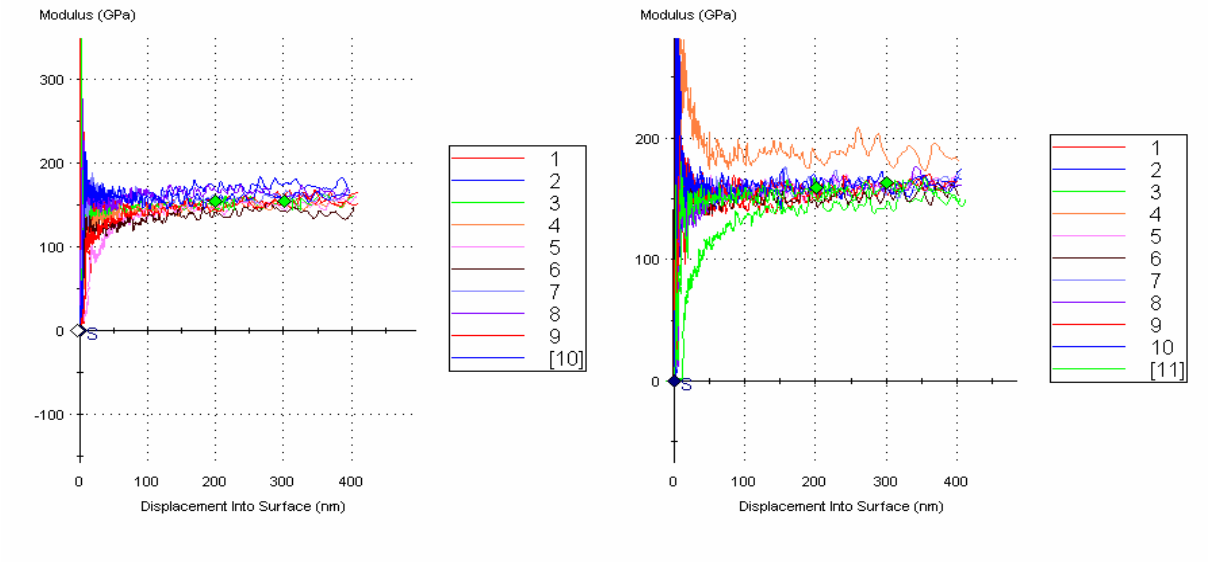

(c) (d)

Fig. 3-6 The measured Young's modulus of case 1. (a) pure Ni-P (b) 0.5g/L diamond (c) 1g/L diamond (d) 2g/L diamond

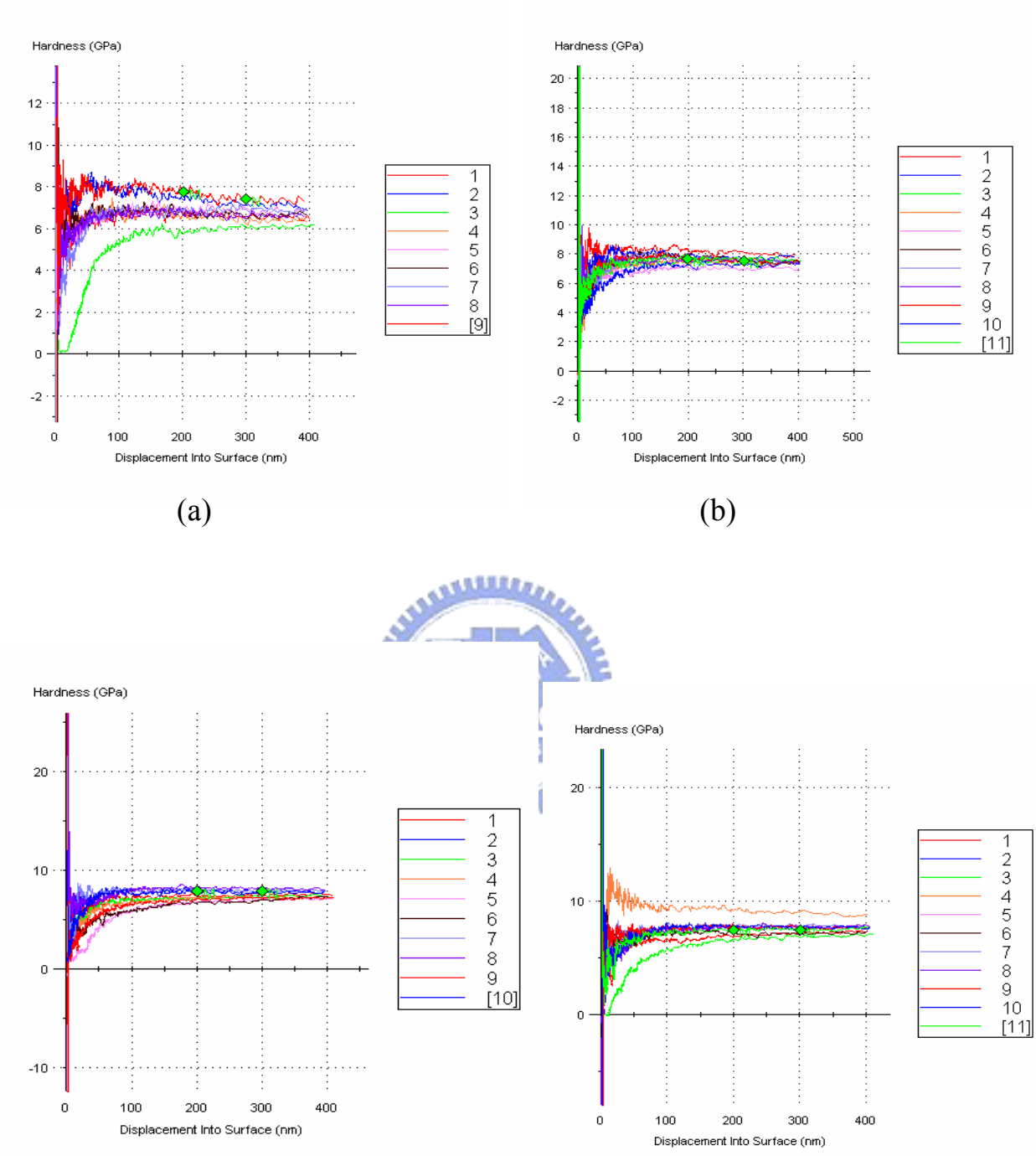

Fig 3-7 The measured hardness of case 1. (a) pure Ni-P (b) 0.5g/L diamond (c) 1g/L diamond (d) 2g/L diamond

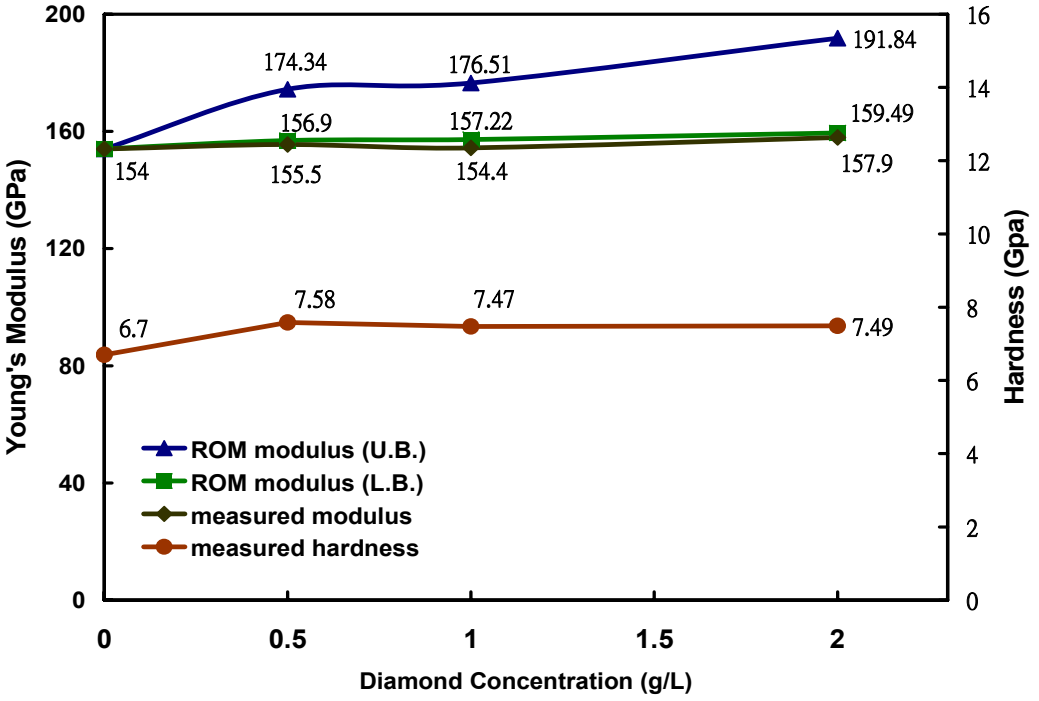

(a)

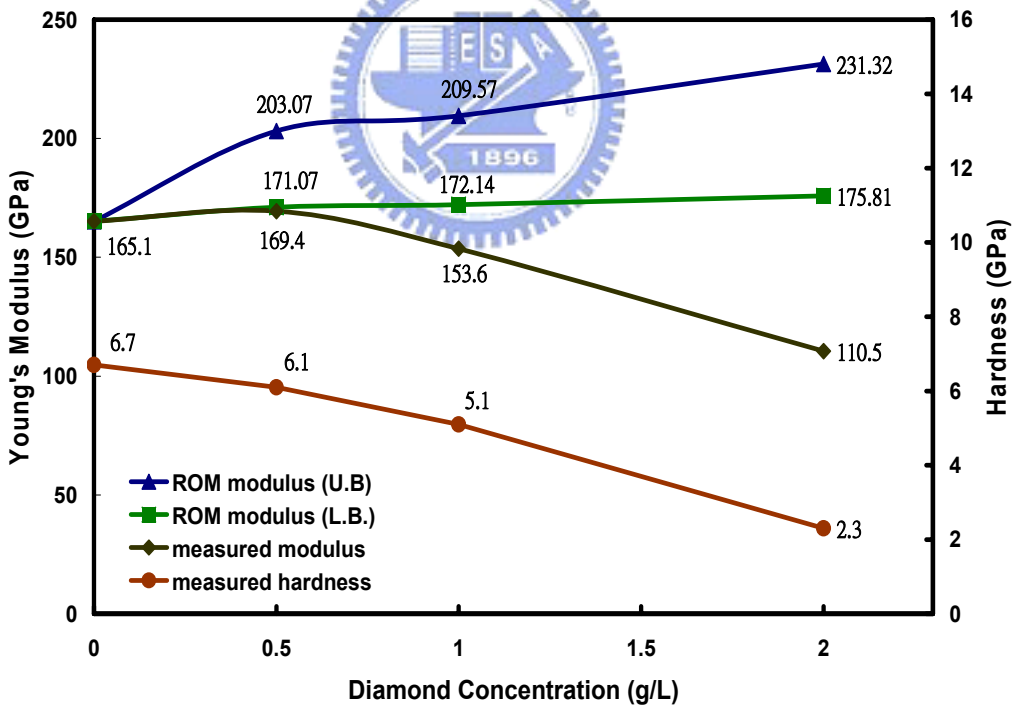

(b)

Fig. 3-8 The comparison of the curves with measured and ROM. (a) case 1 (b) case 2

3.5 Electrical Property Analysis

The 4-point probe is utilized to measure the sheet resistance of the Ni-P-Diamond films. The intrinsic bulk resistivities of EN-based of nanocomposite film are obtained by multiplying the sheet resistance by film thickness. Table 3-2 shows the measurement results. The data shows the resistivity increases with the incorporated diamond powders concentration, because the diamond powder is an insulator that contributes no electrical conductivity to the Ni matrix. Based on the model of two-phase random network, the Maxwell-Wanger equation [19] described in Eq. 1 is utilized for the characterization of the electrical conductivity of the composites.

$$k_c = k_m \frac{1+2V_f(1-k_m/k_d)/(1+2k_m/k_d)}{1-V_f(1-k_m/k_d)/(1+2k_m/k_d)} \qquad (1)$$

Where K_c is the conductivity of the Ni-based composite film, K_m is that of the Ni matrix, K_d that of the second phase composite, V_f the volume fraction of the second phase. Here, Eq. 1 can be approximated in Eq. 2 with $K_m \gg K_d$ for Ni-P-Diamond films, because the diamond is an insulator.

$$k_c = k_m(1-V_f)/(1+V_f/2) \qquad (2)$$

Substituting the know parameters K_m and V_f into the Eq. 2, the conductivity of the Ni-P-diamond films can be obtained and transform it into the resistivity that

shown in the Fig.3-9. We can see that the large discrepancy between the measurement results and theoretical predictions. In case 2, this discrepancy might result from the increase of cracks and voids, but this conjecture is not existence in case 1, what reason to cause this phenomenon should be further discussion.

Table 3-2 The measured sheet resistance and resistivity of Ni-P-Diamond composite films.

	Case 1				**Case 2**			
	Pure Ni	**0.5g/L D**	**1.0g/L D**	**2.0g/L D**	**Pure Ni**	**0.5g/L D**	**1.0g/L D**	**2.0g/L D**
R_s(mΩ/□)	155.2	143.6	150	172.5	310	83.1	94.4	121.6
	146.3	143.6	147.5	171.3	315	85.2	95.8	119.5
	146.2	142.9	147.3	170.9	327	84	106.2	120.4
	146	140.8	146.9	170.7	351	83.3	92.3	113.5
	145.6	139.5	146.7	167.8	349	85.8	94.9	117.4
	145.4	139	146.2	167.2	331	80	93.7	114.2
	145	138.6	145.8	166.9	326	81.6	86.4	110.9
	145	137.6	143.7	165.2	319	84.1	89	104.4
	143.5	137.1	143.4	164.5	346	81.1	86.3	111.6
avg.	146.17	139.68	145.93	167.96	330.4	83.1	93.2	114.8
Film thickness(μm)	5.95	7	7.3	6.7	3.8	16.2	16.3	13.6
Resistivity $\rho(10^{-9}\Omega\text{-m})$	869.71	977.76	1065.3	1125.3	1255.7	1346.8	1519.5	1561.3

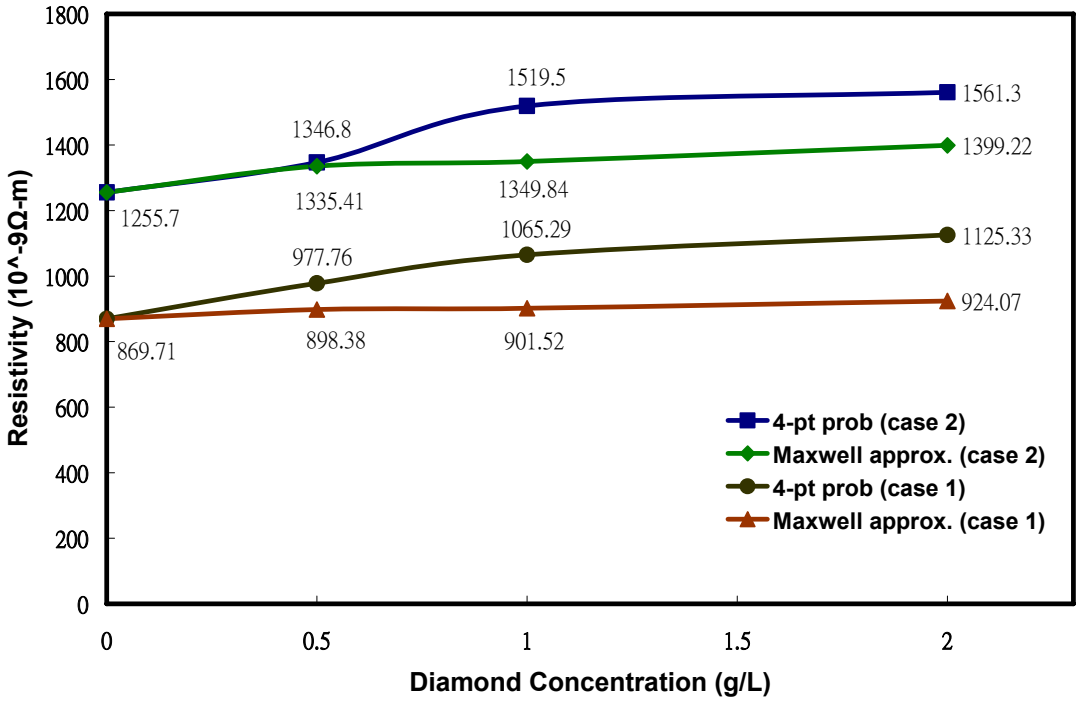

Fig. 3-9 The resistivity versus diamond concentration curve of the Ni-P-Diamond nanocomposite films.

3-6 Displacement Measurements of the electrothermal Microactuator

The measurement results of electrothermal microactuator plated in different concentrations of Ni-P-Diamond plating solutions are shown in Fig. 3-10. In the measurement, different voltages applied on the two anchors to electrically heat the two beams (see in Fig. 2-1). The tip of the beam will curve to the direction of the short beam due to the different elongations result from different beam lengths. The data reveals that the mechanical strength of the actuator made of Ni-P-Diamond nanocomposite has been improve in comparison with that made of the pure Ni-P. Fig. 3-11 shows the measurement results of case 1 and case 2

plated in pure Ni-P and 2g/L Ni-P-Diamond plating bath. We can observe that the maximum displacement of actuator made of 2g/L Ni-P-Diamond can reach 10μm in both cases, which are 1.5 times larger in case 1 and 4 times larger in case 2 than that of the pure one, respectively. Here are different results in power efficiency between with the case 1 and case 2, at the same displacement, the Ni-P-Diamond nanocomposite film has better power efficiency than that of the pure one in case 2, but it is opposite in the case 1. Previously, we have reported the similar investigate in electroplating Ni-Diamond nanocomposite system [20], the measurement result is similar to the case 2 that the Ni-Diamond nanocomposite film has better power efficiency, Fig. 3-12 shows the plot of the measurement results. This difference may result from the different coefficient of thermal expansion (CTE). The measured of CTE values shown in Table 3-3 and is plotted in Fig. 3-13. By the measured displacement of the microactuator and CTE values, we can observe that the power efficiency is proportion to the CTE value. However, compare the case 1 and case 2, the lower trigger power is needed in case 1 than that in case 2 whatever pure Ni-P film or Ni-P-Diamond films.

Here is a question should be study continued that what is the role of the diamond powders play in here. It should be further investigate to understand, why Ni-P-Diamond nanocomposite electrothermal microactuator has longer maximum displacement than that of the pure one.

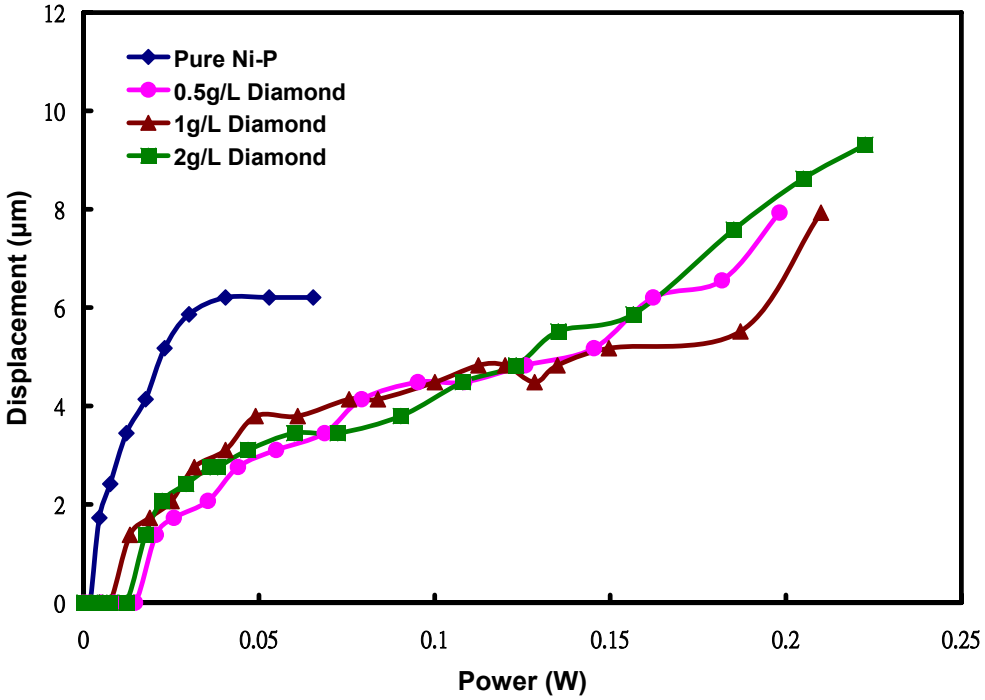

(a)

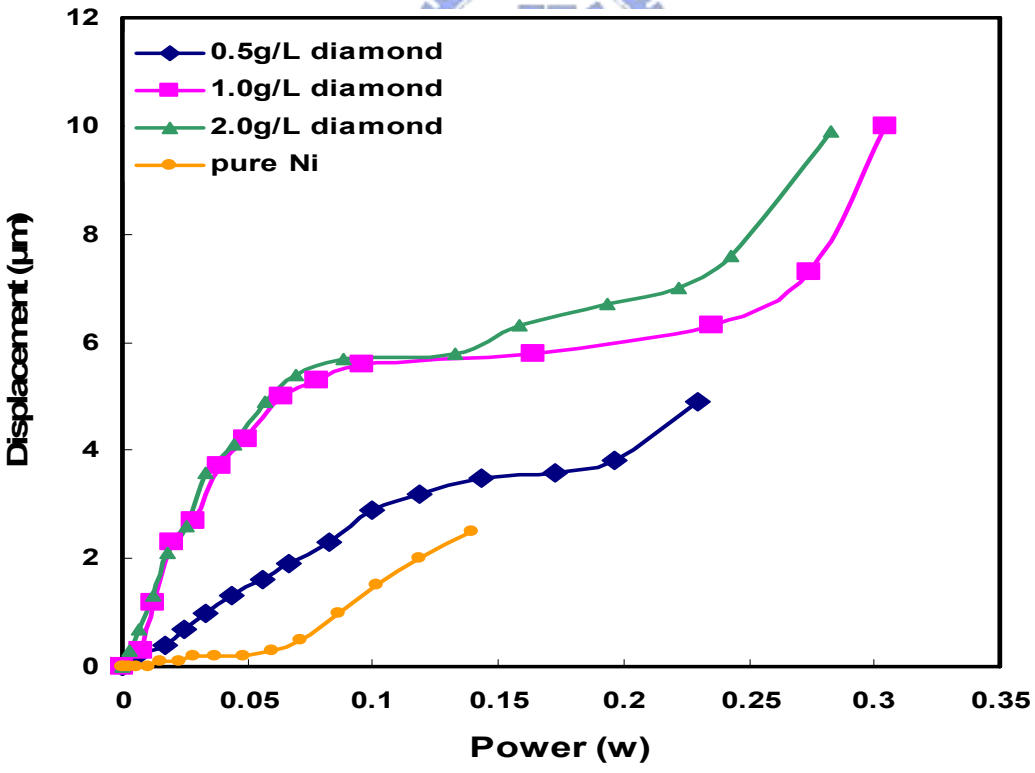

(b)

Fig. 3-10 The diagram of power-displacement for Ni-P-Diamond electrothermal microactuator. (a) Case 1 (b) Case 2

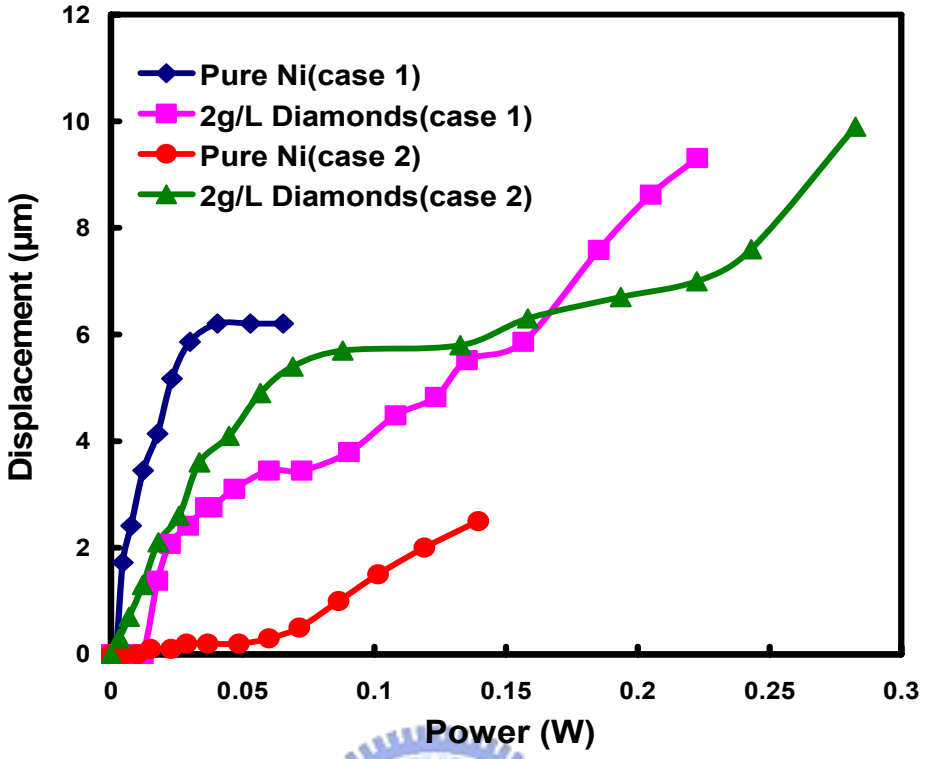

Fig. 3-11 The measured of power-displacement for electrothermal microactuators

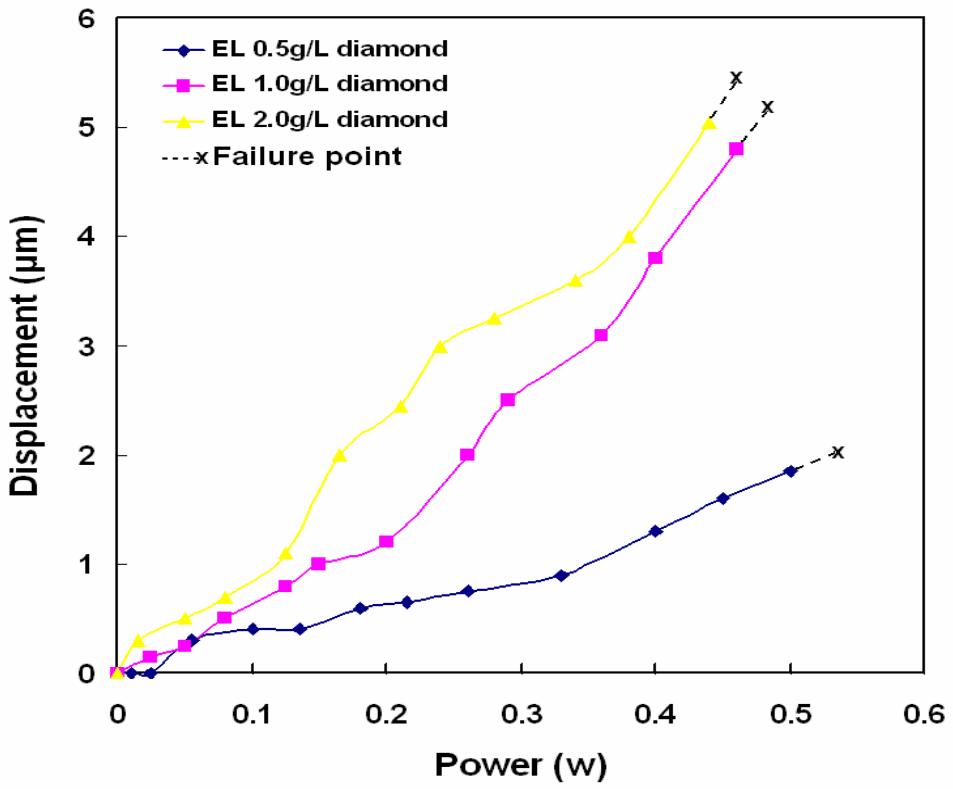

Fig. 3-12 The diagram of power-displacement for electroplating Ni-Diamond electro-thermal microactuators.

Table 3-3 The measured CTE values.

Plating technology	Diamond concentration	CTE (ppm/℃)
Electroless (Case 1)	Pure Ni-P	$13.4*10^{-6}$
	0.5g/L Diamond	$13.19*10^{-6}$
	1g/L Diamond	$13*10^{-6}$
	2g/L Diamond	$10.81*10^{-6}$
Electroplating	Pure Ni	$27*10^{-6}$
	0.5g/L Diamond	$32*10^{-6}$
	1g/L Diamond	$46*10^{-6}$
	2g/L Diamond	$54*10^{-6}$

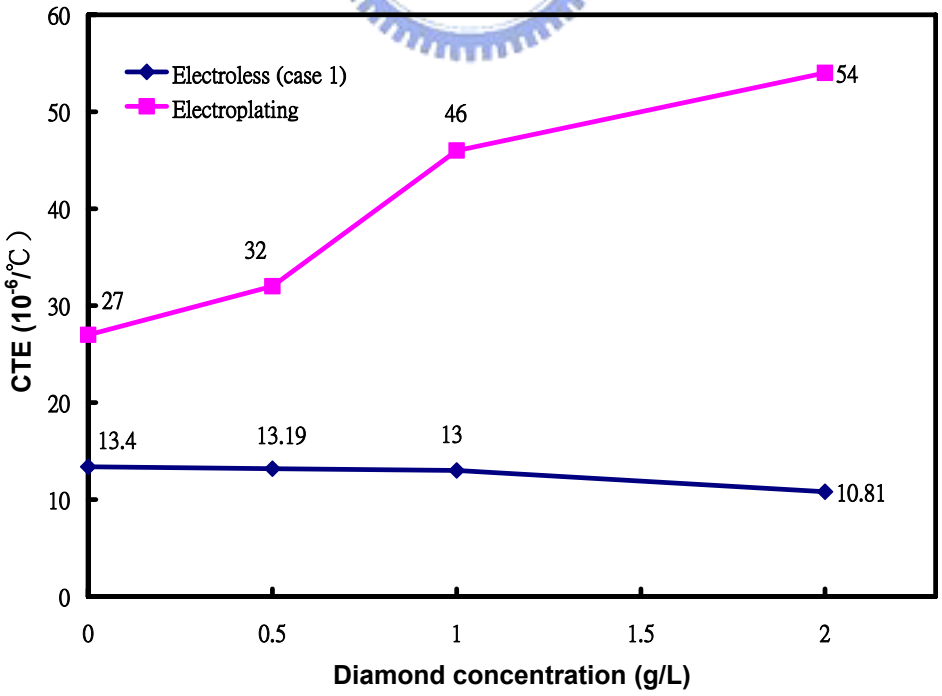

Fig. 3-13 The plot of the measured CTE values.

Chapter 4 Summary and Future Work

4.1 Summary

The properties of different crystallization of Ni-P-Diamond nanocomposites have been reported and compared. According to the mechanical and electrical property analyses and the device characterizations, we found that different crystallization incorporated with the same diamond powders would result in a totally distinct property modification in the Ni-P-Diamond nanocomposite system. By nanoindentation analyze, the amorphous crystallization of Ni-P films incorporated with the nano-diamond powders can improve the Young's modulus and hardness then has better mechanical strength. In contract, the modulus and hardness of the Ni-P films with a mixed microstructure of nanocrystallize and amorphous phase decrease with the incorporation of the nano-diamonds. Furthermore, the measured data of resistivity of the Ni-P-Diamond nanocomposite films reveal that the Ni-P-Diamond nanocomposite with amorphous Ni matrix has better electrical conductivity than the other. Meanwhile, from the displacement measurement of the electrothermal microactuator made of the Ni-P-Diamond composite, it is found that the maximum displacement of the actuator can be improve in both crystallization, and also we can see that the actuator made of the nanocomposite with fully amorphous Ni matrix have better power-efficient performance, in other word, the lower trigger power is needed in the fully amorphous Ni matrix of the pure

Ni-P film and Ni-P-Diamond films.

Finally, the properties of the Ni-P-Diamond nanocomposite with the different microstructure of Ni matrix have been reported. We believe that consider the second phase effect and the matrix microstructure simultaneously, it would be a great helpful to develop a high performance device for application.

4.2 Future Work

So far, we still don't understand what reason it has different crystallization under the same plating solution and fabrication process, this issue is also an argument in other investigator. In order to make a crystallization of EN-based nanocomposite we want, this issue should be clear. Furthermore, in order to further demonstrate the Ni-P-Diamond nanocomposite properties, the other devices such as MEMS resonators and switches should be fabricated and measurement. An excellent performance on the MEMS devices could be expected in the future work.

References

1. K.S. Teh, Y.T. Cheng, and C. Sambucetti," Selective Plating of Nickel Ceramic Composite Films for MEMS Applications" *IEEE Micro Electro Mechanical Systems Conference, Las Vegas, NV*, 2002, pp. 384
2. G..R. Shen, L.N. Tsai, Y.T. Cheng, W. Hsu, and T.K. Lin, "Ni-P-CNTs Nanocomposite Film for MEMS Applications", *IEEE Conference on Nanotechnology, Munchen, Germany*, 2004, pp.192
3. Tzu-Yuan Chao, Guang-Ren Shen, and Y.T. Cheng, "Comparative Study of Ni-P-Diamond and Ni-P-CNT Nanocomposite Films" *accepted to Journal of The Electrochemical Society*, 153 (1)
4. W.X. Chen, J.P. Tu, L.Y. Wang, H.Y. Gan, Z.D. Xu, and X.B. Zhang, "Tribological Application of Carbon Nanotubes in a Metal-based Composite Coating and Composites" *Carbon*, 41(2003), pp.215
5. Céline Nayral, Eric Viala, Pierre Fau, François Senocq, Jean-Claude Jumas, André Maisonnat, and Bruno Chaudret, "Synthesis of Tin and Tin Oxide Nanoparticles of Low Size Dispersity for Application in Gas Sensing" *Chem. Eur. J*., 6(2000), pp.4082
6. Hai Dong, Fuhan Liu, C.P. Wong, "Magnetic Nanocomposite for High Q Embedded Inductor", *9th Int'l Symposium on Advanced Packaging Materials,* 2004, pp.171-174
7. Luisa M. Abrantes, Alda Fundo and Gang Jin, "Influence of Phosphorus Content on the Structure of Nickel Electroless Deposits" *J. Mater. Chem.*, 11(2001), pp.200-203.
8. P. Sampath Kumar and P. Kesavan Nair, "Studies on Crystallization of Electroless Ni-P Deposits", *Journal of Materials Processing Technology,* 56(1996), pp.511-520.
9. K.G. Keong, W. Sha, S. Malinov, "Crystallisation Kinetics and Phase Transformation Behaviour of Electroless Nickel-Phosphorus Deposits with High Phosphorus Content", *J. Alloys Compd.*, 334(2002), pp.192-199.
10. K.G. Keong, W. Sha, S. Malinov, "Crystallization and Phase Transformation Behaviour of Electroless Nickel-Phosphorus Deposits with Low and

Medium Phosphorus Contents Under Continuous Heating“, *Journal of Materials Science*, 37(2002), pp.4445-4450.

11. N.M. Martyak, K. Drake, “Peak-profile Analysis of Electroless Nickel Coatings“, *J. Alloy. Compd.*, 312(2000), pp.30-40.
12. N.M. Martyak, “Characterization of Thin Electroless Nickel Coatings”, *Chem. Mater.*, 6(1994), pp.1667.
13. C.S. Pan, Wen Syan Hsu, “An Electro-Thermally and Laterally Driven Polysilicon Microactuator”, *J. Micromech. And Microeng*., 7(1997), pp.7-13
14. Sheng Hung Chemical Engineering Co., Ltd., http://www.schccl.com.tw
15. Guang-Ren Shen, “Properties Enhancements of Ni-P-CNTs and Ni-P-Diamond Nanocomposites Films and the Applications on MEMS Device”, Master Thesis, National Chiao-Tung University, 2004
16. W. D. Callister, Jr., “Materials Science and Engineering, 3rd Ed.”, Chapter 17, John Wiley and Sons Inc., 1994, pp. 516-521
17. George E. Dieter, “Mechanical Metallurgy, 3rd Ed.”,Chapter 6, McGraw-Hill Book Company, New York, 1978, pp. 184-240
18. Hyoung Seop kim, “On the Rule of Mixtures for the Hardness of Particle Reinforced Composites”, *Materials Science and Engineering A*, 289(2000), pp.30-33
19. Dae Gon Han, and Gyeong Man Choi, “Computer Simulation of the Electrical Conductivity of Composites: the Effect of Geometrical Arrangement”, *Solid State Ionics*, 106(1998), pp.71-87
20. Li-Nuan Tsai, Guang-Ren Shen, Y.T. Cheng, and Wensyang Hsu, “Power and Reliability Improvement of an Electro-Thermal Microactuator Using Ni-Diamond Nanocomposite”, *IEEE ECTC*, *Las Vegas*, 2004, pp.472-476

Vita

姓　　名：蔣宜達（I-Ta Chiang）

出生日期：中華民國六十七年十月四日

出 生 地：台灣省台北縣

E - mail：nettson.ee92g@nctu.edu.tw

學　　歷：

國立淡水商工電子科　　(1993.9～1996.6)
(National Tam-Shui Vocational High School)

私立景文技術學院電子科　　(1996.9～1998.6)
(Jin Wen Institute of Technology)

國立交通大學電子工程所碩士班　　(2003.9～2006.1)
(Department of electronics Engineering & Institute of Electronics, Nation Chiao Tung University)